
STATISTICAL, NONLINEAR,
AND SOFT MATTER PHYSICS

Orientalional Instability in a Nematic Liquid Crystal in a Decaying Poiseuille Flow

S. V. Pasechnik^{a,*}, A. P. Krekhov^b, D. V. Shmeleva^a,
I. Sh. Nasibullaev^b, and V. A. Tsvetkov^a

^aState Academy of Instrument-Making and Informatics, Moscow, 107846 Russia

^bInstitute of Molecular and Crystal Physics, Ural Research Center, Russian Academy of Sciences, Ufa, 450075 Russia

*e-mail: s-p-a-s-m@hotmail.ru

Received August 9, 2004

Abstract—The results of studies of orientational dynamics and instability in an MBBA nematic liquid crystal in a decaying Poiseuille flow are considered. The experiments were made on a wedge cell with a gap width varying in a direction perpendicular to the flow. Confining surfaces ensured homeotropic adhesion of the nematic to the surface. Above a certain critical value of the initial pressure drop, a uniform orientational instability is observed, which corresponds to the emergence of the director from the plane of the flow. The dependence of the critical pressure drop on the local thickness of the liquid crystal layer and on the external destabilizing electric field is determined. Simulation of nematodynamics equations is carried out. The results of theoretical calculations are in qualitative and quantitative agreement with the experimental data. © 2005 Pleiades Publishing, Inc.

1. INTRODUCTION

Nematic liquid crystals are anisotropic liquids characterized by orientational ordering of molecules. These bodies can serve as a model system for studying universal regularities of rheological behavior of various complex liquids such as liquid-crystal polymers, lamellar phases of solutions of surfactants, and melts of block-copolymers. Specific features in the behavior of a liquid crystal in a flow are determined by anisotropy of viscoelastic properties and by the interaction between the field of velocity \mathbf{v} and the average local orientation of molecules, which is described by a unit vector (director) \mathbf{n} . Orientational instabilities in a nematic flow have been studied most comprehensively for the case when the initial orientation of the director is perpendicular to the plane of the flow [1–3]. Theoretical analysis of a steady-state Poiseuille flow with a homeotropic orientation of the director at the boundary surfaces of the layer (vector \mathbf{n} is perpendicular to the surface) shows that an increase in the gradient of pressure applied along the layer above a certain critical value leads to uniform orientational instability accompanied by the emergence of the director from the plane of the flow [4]. An analogous instability, which was predicted for an oscillating Poiseuille flow [5], was observed earlier and studied experimentally at frequencies from 1 to 20 Hz [6]. At small amplitudes of a decaying Poiseuille flow in a liquid crystal with an initial homeotropic orientation, the director field in the plane of the flow is distorted [7]. However, the stability of such a state upon an increase in the initial pressure drop has not been studied experimentally as yet.

Here, we report on the results of a study of the orientational behavior and instabilities in an MBBA (*n*'-methoxybenzylidene-*n*-butylaniline) nematic liquid crystal under the action of a decaying Poiseuille flow. The effect of a destabilizing electric field on the orientational instability threshold is investigated.

2. EXPERIMENT

The experimental cell is shown schematically in Fig. 1. A capillary with a wedge gap was formed by glass plates with inner surfaces coated with a thin conducting SnO₂ layer, which made it possible to apply an electric field to the liquid crystal layer. The treatment of the surfaces with chromolane ensured a homeotropic (perpendicular to the surface) orientation of the nematic on the substrates. The main feature of the cell was wedge-shaped with a local layer width h varying along the y axis. The linearity of the $h(y)$ dependence and the absolute values of local width h were monitored from the variation of the phase difference between the ordinary and extraordinary rays caused by a decrease in the alternating voltage ($U_0 = 45$ V, a frequency of 5 kHz) applied to the MBBA layer to zero [8]. The absolute error in determining the local width h was approximately 2–3 μm . Prior to the experiment, the cell was mounted vertically and was filled with the liquid crystal so that the material filled the capillary, filling channels, and a part of expansion vessels (cylindrical pipes of diameter D). Decaying Poiseuille flow (along the x axis) was produced because of introduction of the crystal into one of expansion vessels. The initial pressure

drop ΔP_0 created in this case and proportional to the initial difference ΔH_0 in the levels of the liquid crystal was calculated to within 5% from the mass of the crystal introduced in the cell and the diameter of the expansion vessels. The experiments were carried out at temperature $T = 22 \pm 0.5^\circ\text{C}$.

For a small wedging,

$$(h_{\max} - h_0)/A \approx 0.002,$$

the capillary can be treated as a set of channels having different widths and parallel to the x axis, to which the same pressure gradient $\Delta P/L$ is applied. In addition, in view of the large aspect ratio of the cell,

$$\frac{A}{(h_{\max} + h_0)/2} \approx 800, \quad \frac{L}{(h_{\max} + h_0)/2} \approx 80,$$

we can expect that a plane Poiseuille flow along the x axis is formed in the capillary (except for the boundary regions at the ends of the cell); this is confirmed by observations of movement of small impurity particles ($2\text{--}4\ \mu\text{m}$ in diameter) added to the nematic.

The intensity $I(t)$ of light with a wavelength of $628\ \text{nm}$ (He-Ne laser) transmitted (along the z axis) through the capillary was detected from an area of diameter $D = 0.3\ \text{mm}$ by a photodiode and recorded in digital form (with the help of A to D converter) on the hard disk of a computer. Two versions of positions of the polarizer and the analyzer were used in the experiment: crossed polaroids oriented at an angle of $\alpha = 45^\circ$ to the direction of the flow (geometry a) and at an angle of $\alpha = 0^\circ$ (geometry b). Geometry b made it possible to detect the emergence of the director from the xz plane of the flow. Shadow images of the cell in crossed polaroids in geometries a and b were recorded simultaneously with the help of a digital camera.

3. EXPERIMENTAL RESULTS

For small initial pressure drops ($\Delta P_0 \leq 6\ \text{Pa}$) in the entire range of local cell thicknesses $h_0 < h < h_{\max}$, no changes in the intensity of transmitted light were detected in the b geometry; consequently, the director preserved its orientation in the plane of the flow. In the a geometry, this regime corresponds to the shadow image of the cell, consisting of dark and bright fringes arranged along the direction of the flow and formed as a result of interference of the ordinary and extraordinary rays. The phase delay appears as a result of a change in the refractive index, which is in turn associated with a deviation of the director from the initial homeotropic orientation. The dynamics of the interference fringes is as follows: the formation of the fringe structure in the region of large local thicknesses begins immediately after the emergence of the initial pressure difference; after this, the system of fringes moves

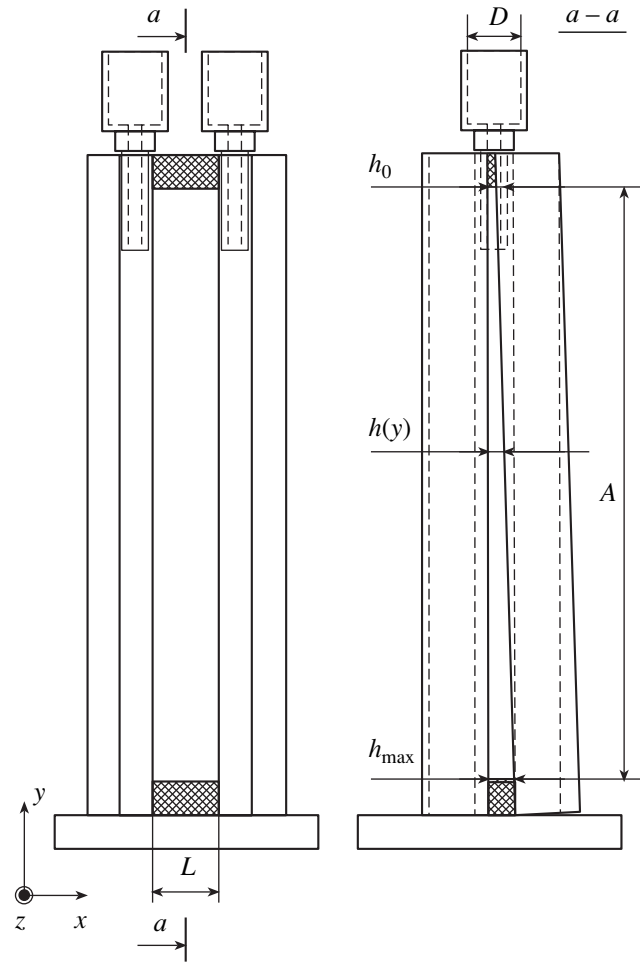


Fig. 1. Geometry of a wedge-shaped cell: $A = 10\ \text{cm}$, $L = 1\ \text{cm}$, $h_{\max} = 210\ \mu\text{m}$, $h_0 = 33\ \mu\text{m}$, and $D = 1.5\ \text{cm}$.

towards smaller thicknesses. In the steady-state decaying Poiseuille flow, the fringes slowly move towards larger thicknesses.

Recording the intensity of transmitted light locally in the a geometry,

$$I(t) = I_0 \sin^2[\delta(t)/2],$$

where I_0 is the input intensity, we found that the phase lag $\delta(t)$ decreases exponentially with time (curve I in Fig. 2). For small deviations of the director (in the plane of the flow) from the initial homeotropic orientation, we can derive the following time dependence of the phase lag [7]:

$$\begin{aligned} \delta(t) &= \delta_0 \exp(-t/\tau_\delta), \quad \tau_\delta = \eta_{\text{hom}}/\rho g k_0, \\ k_0 &= A(h_{\max} + h_0)(h_{\max}^2 + h_0^2)/3\pi D^2 L, \end{aligned} \quad (1)$$

where δ_0 is the maximal value of the phase lag at the

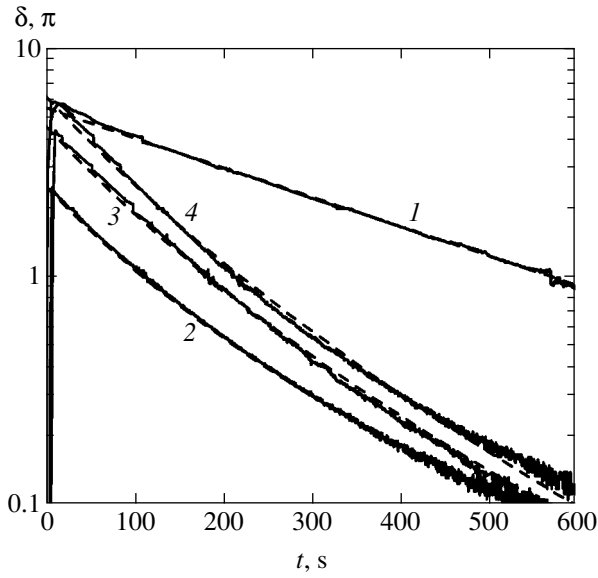


Fig. 2. Time dependence of the phase lag $\delta(t)$. Experimental data (solid curves) and results of simulation (dashed curves): $\Delta P_0 = 1.5$ Pa, $h = 164$ μm (1), $\Delta P_0 = 9.4$ Pa, $h = 70$ μm (2), $\Delta P_0 = 12.8$ Pa, $h = 70$ μm (3), and $\Delta P_0 = 15.5$ Pa, $h = 70$ μm (4).

instant of stabilization of the decaying flow,

$$\eta_{\text{hom}} = \frac{-\alpha_2 + \alpha_4 + \alpha_5}{2}$$

is the viscosity of the homeotropically oriented liquid crystal, ρ is the density of the nematic, g is the acceleration due to gravity, and k_0 is a quantity constant for the given cell and depending on the geometrical size. The experimental data for $\delta(t)$ are correctly described by dependence (1) using η_{hom} as a fitting parameter. The value of $\eta_{\text{hom}} = 0.16 \pm 0.02$ Pa s obtained for MBBA is in good agreement with the results of independent measurements [9, 10]. Our experiments suggest a new simple and reliable technique for measuring the viscosity coefficients of nematic liquid crystals, which is based on the recording of the time dependence of the phase lag in a decaying Poiseuille flow. If the cells used in experiments ensure the planar boundary conditions (the director is oriented parallel to the substrates in the plane of the flow), it is possible to measure the viscosity

$$\eta_{\text{plan}} = \frac{\alpha_3 + \alpha_4 + \alpha_6}{2}.$$

With increasing initial pressure drop ($\Delta P_0 > 6$ Pa), the signal intensity $I(t)$ of transmitted light in the b geometry, which is recorded in the range of large thicknesses of the cell, exhibits two peaks (curve 2 in Fig. 3a), indicating the emergence of the director from the plane of the flow. Figure 3b shows the theoretical dependences $I(t)$ in geometries a and b as well as the

angle $\phi_m(t)$ of deviation of the director from the plane of the flow at the center of the layer. The nonlinear nematodynamics equations [11] for a planar layer, when the director and the velocity are functions of coordinate z and time t [12], were solved numerically using the material parameters for MBBA [10, 13]. The intensity of transmitted light was calculated using the Jones matrix method [14, 15]. Angle ϕ_m characterizes the orientation of the director at the center of the layer:

$$\mathbf{n}_m = (0, \sin \phi_m, \cos \phi_m).$$

The director distribution at the instant corresponding to $\phi_m = 60^\circ$ is shown in Fig. 3c. The first peak of the $I(t)$ signal in the b geometry is associated with the emergence of the director from the plane of the flow in the case of a large initial pressure drop. As the pressure drop $\Delta P(t)$ decreases below the threshold value, the director returns to the plane of the flow (second peak on the $I(t)$ curve in the b geometry) and relaxes over long time periods to the uniform homeotropic orientation.

The transition associated with the emergence of the director from the plane of the flow is observed most clearly in the shadow image of the cell (Fig. 4). In the b geometry (Fig. 4b), the shadow image is (in the increasing order of the local layer thickness) dark field I in the range of smaller thicknesses, light fringe II, and the low-intensity region III. In the a geometry (Fig. 4a), two regions can be clearly distinguished on the shadow image: region I + II, corresponding to relatively small thicknesses, in which wide interference fringes parallel to the direction of the flow are observed, and region III, corresponding to large thicknesses, where narrow interference fringes are transformed into wide fringes.

The polarization and optical analysis, as well as a comparison of microphotographs (Fig. 4) with the time dependences of transmitted light (Fig. 3a), make it possible to unambiguously identify all regions on the shadow image of the cell: region I (the director is in the plane of the flow, the azimuth angle ϕ_m of deviation of the director at the center of the layer is zero); region II (the director emerges from the plane of the flow ($0 < \phi_m < 20^\circ$)), and region III (the director is oriented almost perpendicularly to the plane of the flow, $\phi_m \rightarrow 90^\circ$).

The recording of shadow images and the intensity of transmitted light in the b geometry made it possible to clarify the nature of formation of the region corresponding to the emergence of the director from the plane of the flow. Immediately after the application of the initial pressure gradient (for 10–15 s) in the range of large values of local thicknesses of the nematic layer, light fringe II is formed, which subsequently moves along the y axis towards smaller thicknesses over a time of approximately 30–40 s. After approximately 50–60 s, the position of the light fringe stabilizes, and the fringe begins to move slowly in the direction of increasing layer thickness. This stage corresponds to a steady-state decaying Poiseuille flow. The boundary y_b

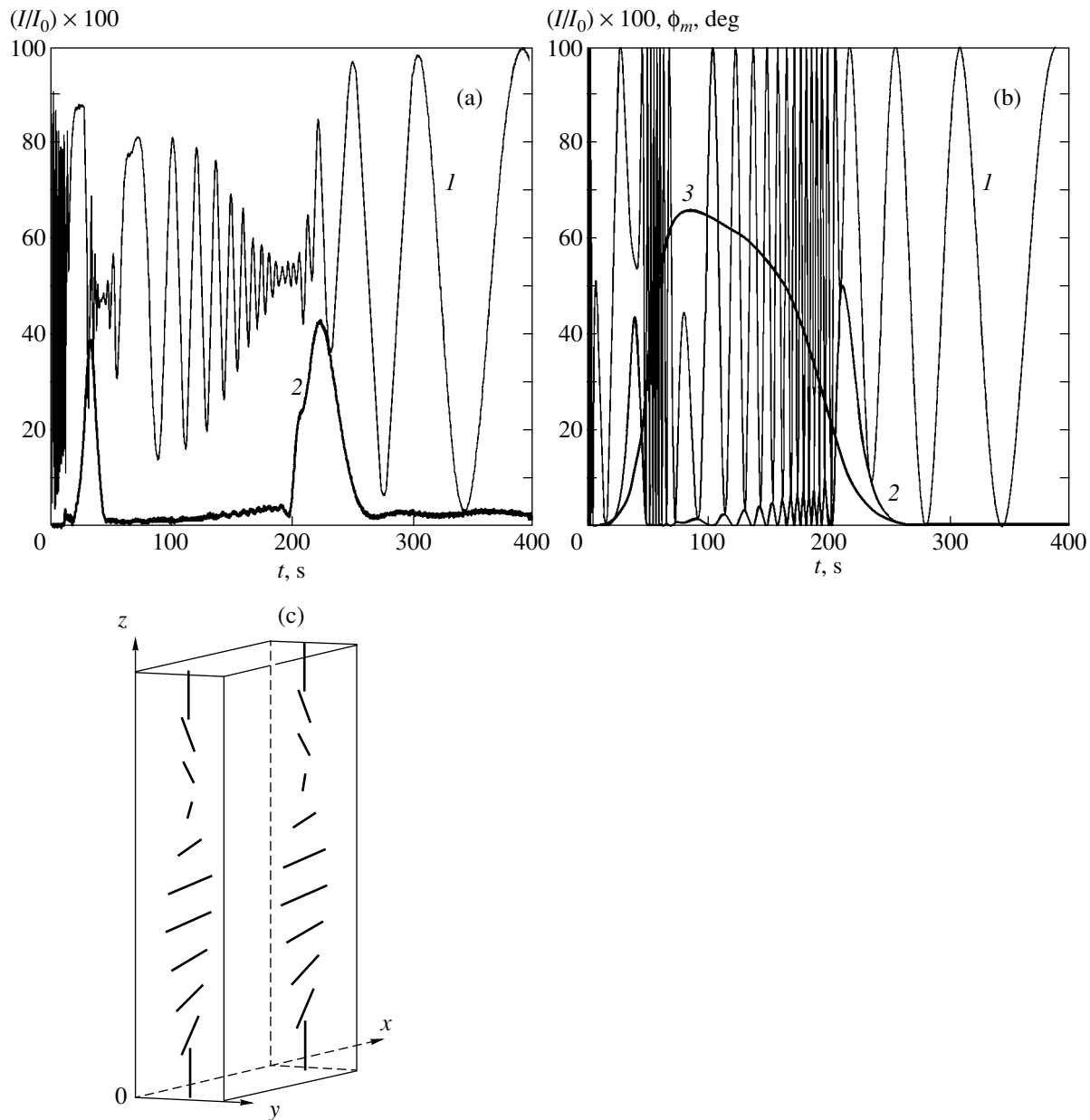


Fig. 3. Time dependences of the intensity of transmitted light, $I(t)$, in geometry *a* (curves 1) and *b* (curves 2) and of the angle of deviation of the director from the plane of the flow at the center of the layer, $\phi_m(t)$ (curve 3). (a) Experimental data: $\Delta P_0 = 20$ Pa, $h = 86$ μm ; (b) theoretical calculations: $\Delta P_0 = 21$ Pa, $h = 90$ μm ; (c) schematic diagram of orientation of the director at the instant corresponding to $\phi_m = 60^\circ$.

between regions II and III can be seen most clearly, while the boundary between regions I and II becomes less clear as fringe II moves towards large thicknesses. The width of region II attains its minimal value when it begins its reverse motion and increases as fringe II moves towards large local thicknesses. The presence of two peaks in the $I(t)$ signal in the *b* geometry (Fig. 3a) is due to the fact that light fringe II passes twice through the point of observation.

At the stage corresponding to a steady-state decaying Poiseuille flow, we recorded the time dependence

$y_b(t)$ of the position of the boundary between regions II and III since this boundary remains the clearest during the entire experiment. The simultaneous recording of the phase lag $\delta(t)$ in the *a* geometry in the range of small local widths of the liquid crystal layer makes it possible to reconstruct the time dependence of the pressure drop, $\Delta P(t)$. Since the director is oriented in the plane of the layer in the range of small local thicknesses of the layer (the absence of signal $I(t)$ in the *b* geometry) and deviations from the homeotropic orientation are small, the measured phase lag is proportional to the square of

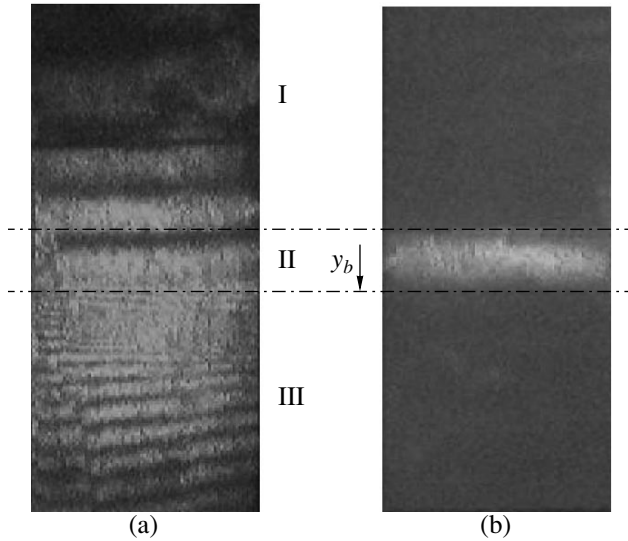


Fig. 4. Shadow images of the cell in crossed polaroids at instant $t = 30$ s for $\Delta P_0 = 15.5$ Pa: (a) in geometry a ; (b) in geometry b .

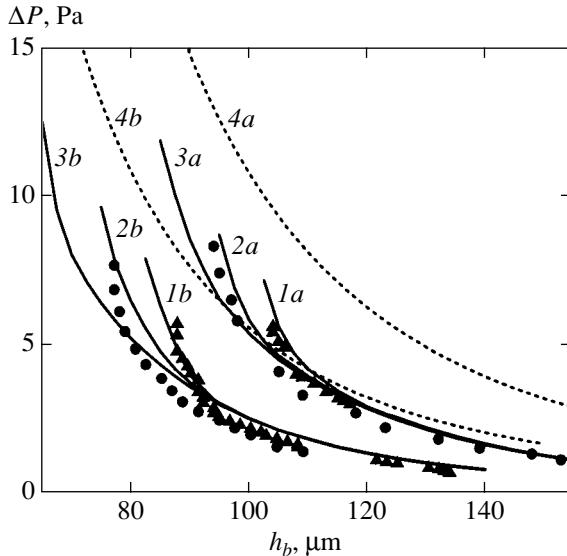


Fig. 5. The threshold pressure drop ΔP_c corresponding to the emergence of the director from the plane of the flow as a function of the local layer thickness h_b . Experimental data are shown by symbols and the results of calculations are given by curves. $U = 0$: $\Delta P_0 = 9.4$ Pa (\blacktriangle and $1a$), $\Delta P_0 = 12.8$ Pa (\bullet and $2a$), $\Delta P_0 = 15.5$ Pa (\blacksquare and $3a$); $U = 3$ V: $\Delta P_0 = 8.7$ Pa (\blacktriangle and $1b$), $\Delta P_0 = 10.8$ Pa (\bullet and $2b$), and $\Delta P_0 = 14.1$ Pa (\blacksquare and $3b$). Curves $4a$ and $4b$ correspond to calculations for the case of a steady-state Poiseuille flow for $U = 0$ and 3 V, respectively.

the pressure drop [16],

$$\delta(t) \sim [\Delta P(t)]^2,$$

which makes it possible to calculate $\Delta P(t)$ from the corresponding dependence $\delta(t)$. It should be noted that, for large initial pressure gradients, the time dependences

$\delta(t)$ of the phase lag differ substantially from the simple exponential law (1) (curves 2, 3, and 4 in Fig. 2). This is due to the fact that, after the application of a large initial pressure gradient, the orientation of the director becomes almost perpendicular to the plane of the flow in the major part of the cell, and the director returns to the plane of the flow in the course of deceleration, after which it acquires the equilibrium homeotropic orientation; as a result, the effective viscosity of the nematic varies with time. For this regime of the flow, we can derive the following semi-empirical expression for $\delta(t)$:

$$\delta(t) = \delta_0 \exp[-t/\tau_\delta(t)],$$

$$\tau_\delta(t) = \frac{\eta_{\text{hom}} - (\eta_{\text{hom}} - \eta_{\text{per}}) \exp(-t/\tau_0)}{\rho g k_0}, \quad (2)$$

with a slowly varying relaxation time $\tau_\delta(t)$. In expression (2),

$$\eta_{\text{per}} = \alpha_4/2$$

is the viscosity of the liquid crystal oriented perpendicularly to the plane of the flow and τ_0 is a fitting parameter. The relative variation of the relaxation time,

$$\frac{\tau_\delta(0)}{\tau_\delta(\infty)} = \frac{\eta_{\text{per}}}{\eta_{\text{hom}}},$$

is associated with the change in the orientation of the director from the orientation perpendicular to the plane of the flow to the homeotropic orientation. For MBBA at $T = 22^\circ\text{C}$, we have $\eta_{\text{per}}/\eta_{\text{hom}} = 0.31$ [10]. It can be seen from Fig. 2 (curves 2, 3, and 4) that the experimental data are correctly described by dependence (2) for various initial pressure gradients.

Thus, using the data on the time dependence $y_b(t)$ of the position of the boundary and the dependence $\Delta P(t)$ reconstructed from $\delta(t)$, we can associate the value of pressure drop with the position of boundary y_b recorded in the experiment, thus establishing the dependence of the critical pressure gradient ΔP_c , corresponding to the emergence of the director from the plane of the flow, on local thickness h_b of the liquid crystal layer. Figure 5 (curves marked by a) shows the $\Delta P_c(h_b)$ dependence obtained for various values of the initial pressure drop ΔP_0 . It can be seen from the figure that, for large values of h , the curves obtained for different values of ΔP_0 almost coincide. This is due to the fact that large thicknesses correspond to large time intervals following the application of the initial pressure drop, when a quasi-stationary flow sets in the cell. The velocity varies slowly with time and the director can follow the variation of pressure. Accordingly, the position of the boundary y_b in such a flow regime is determined only by the current value of ΔP and does not depend on ΔP_0 .

The results of analysis of the effect of an electric field applied along the z axis on the threshold for the emergence of the director on the plane of the flow are given by curves marked by b in Fig. 5. The reduction of the critical value $\Delta P_c(h_b)$ is due to the fact that the electric field exerts a destabilizing effect (in addition to the flow) on the homeotropically oriented MBBA layer (negative anisotropy of permittivity).

Figure 5 also shows the theoretical $\Delta P_c(h_b)$ dependences obtained from the results of simulation of the nonlinear nematodynamics equations [11] for the case when the director and velocity are functions of coordinate z and time t [12] using the material parameter of MBBA [10, 13]. For a number of values of thickness of a planar layer of the liquid crystal, the orientational dynamics of the director was calculated using the experimentally determined time dependence $\Delta P(t)$ of the pressure drop. At the initial instant, the director is oriented homeotropically and emerges from the plane of the flow when the value of ΔP exceeds a certain critical value (depending on the thickness). As the pressure decays, the director returns to the plane of the flow. The threshold value ΔP_c corresponds to the instantaneous value $\Delta P(t)$ at which the return of the director to the plane of the flow is registered. The results are in good agreement with the experimental data considering that the wedge-shape cell was simulated in numerical calculations by a set of planar capillaries, taking into account experimental errors in determining ΔP_c and h_b .

Figure 5 also shows for comparison the dependences $\Delta P_c^{\text{st}}(h)$ of the critical pressure drop corresponding for the emergence of the director from the plane of the flow, which were calculated for a steady-state Poiseuille flow (curves 4). The critical value of the pressure drop for a steady-state Poiseuille flow,

$$\Delta P_c^{\text{st}} \sim 1/h^3,$$

systematically exceeds the corresponding values of ΔP_c for a decaying flow. This is due to the fact that the return of the director to the plane of the decaying flow occurs upon a decrease in pressure $\Delta P(t)$ below ΔP_c^{st} over a finite time (on the order of the director relaxation time), during which the pressure continues to decrease.

The wedge-shaped structure of the cell enabled us to observe the behavior of a liquid crystal in a wide range of thicknesses in the same experiment. It was found that at thicknesses exceeding the threshold values for the emergence of the director from the plane of the flow, regions (domains) of various shape and size were formed. A characteristic feature of these domains is their long lifetime. For example, for a layer having a thickness of about 130 μm and $\Delta P_0 \approx 25$ Pa, the time of relaxation of the director to the original homeotropic orientation in these domains is longer than 3 h, which exceeds the characteristic time of flow decay (<10 min)

and the time of restoration of the initial orientation outside these domains.

In polarized monochromatic light, in the a geometry, the interference pattern in the domains is similar to that described above, but inclined interference fringes in this case move at a much lower velocity. In the b geometry, these domains have an average illuminance higher than that of neighboring regions of the cell. At times exceeding the flow decay time, the domains are successfully visualized against the background of the dark field corresponding to the homeotropic orientation and are separated from the latter by a bright threadlike boundary (domain wall). The boundary of the regions is also observed for the position of both polaroids parallel to the direction of the flow. In this case, it separates two regions with equal illuminances.

The domains were formed over approximately 1–2 minutes after the generation of the flow in the form of one or several formations oriented along the flow. The area of the domains is the larger, the higher the initial pressure drop ΔP_0 . For large values of the initial pressure gradient, a single region occupying a substantial part of the cell was formed.

It should be noted that domains are formed for thicknesses $h > h_b$, i.e., at velocities exceeding the threshold value for the emergence of the director from the plane of the flow. Consequently, the formation of domains can be treated as the result of secondary hydrodynamic instabilities developing against the background of a strongly deformed structure of the layer associated with the primary instability. In the central regions of the layer, for large pressure drops, a distribution close to that perpendicular to the plane of the flow is formed for the director as a result of primary instability (Fig. 3c). For such an orientation, the same mechanisms affect the stability of the director as those considered in [2, 17] for the initial orientation perpendicular to the plane of the flow. However, the mechanism of formation of these domains with anomalously long lifetime remains unclear and requires further investigations.

4. CONCLUSIONS

Oriental instability formed in a nematic liquid crystal under the action of a decaying Poiseuille flow and accompanied by the emergence of the director from the plane of the flow is detected experimentally and studied for the first time. The development of instability is visualized in a wedge-shaped cell in the form of a sharp boundary (domain wall) separating spatial regions in which the orientation of the director is in the plane of the flow and outside this plane. Analysis of the dynamics of motion of the domain wall in a decaying flow made it possible to determine the dependence of the threshold pressure drop on the thickness of the liquid crystal layer. It is found that the additional action of an electric field on the nematic layer with a negative

anisotropy of the permittivity lowers the threshold for the emergence of the director from the plane of the flow. The results of theoretical calculations of the critical pressure drop are in quantitative agreement with the experimental data. The analysis of the orientational behavior of the director in a decaying Poiseuille flow has demonstrated the possibility of determining the viscosity coefficients of the nematic to a high degree of accuracy from the data on the optical response for small initial pressure gradients.

ACKNOWLEDGMENTS

The authors are grateful to O.S. Tarasov for fruitful discussions of the results and for a critical review of the article.

This study was supported by the Russian Foundation for Basic Research (project no. 02-02-17435), Federal Target Program "Integration" (grant no. B0065), INTAS (grant no. YSF 01/1-188), and DAAD (grant no. 325 A/03/01330).

REFERENCES

1. P. Pieranski and E. Guyon, *Phys. Rev. A* **9**, 404 (1974).
2. E. Guyon and P. Pieranski, *J. Phys. Colloq.* **36**, C1-203 (1975).
3. E. Dubois-Violette and P. Manneville, in *Pattern Formation in Liquid Crystals*, Ed. by A. Buka and L. Kramer (Springer, New York, 1996), p. 91.
4. I. Zuniga and F. M. Leslie, *J. Non-Newtonian Fluid Mech.* **33**, 123 (1989).
5. A. P. Krekhov and L. Kramer, *J. Phys. II* **4**, 677 (1994).
6. P. Toth, A. P. Krekhov, L. Kramer, and J. Peinke, *Europhys. Lett.* **51**, 48 (2000).
7. S. V. Pasechnik, V. A. Tsvetkov, A. V. Torchinskaya, and D. O. Karandashov, *Mol. Cryst. Liq. Cryst.* **366**, 165 (2001).
8. W. De Jeu, *Physical Properties of Liquid Crystalline Materials* (Gordon and Breach, New York, 1980; Mir, Moscow, 1982).
9. H. Knepe and F. Schneider, *Mol. Cryst. Liq. Cryst.* **65**, 23 (1981).
10. H. Knepe, F. Schneider, and N. K. Sharma, *J. Chem. Phys.* **77**, 3203 (1982).
11. P.-G. de Gennes, *The Physics of Liquid Crystals* (Clarendon, Oxford, 1974; Mir, Moscow, 1977).
12. A. P. Krekhov and L. Kramer, *Phys. Rev. E* **53**, 4925 (1996).
13. W. H. de Jeu, W. A. P. Claassen, and A. M. J. Spruijt, *Mol. Cryst. Liq. Cryst.* **37**, 269 (1976).
14. T. J. Scheffer and J. Nehring, *J. Appl. Phys.* **56**, 908 (1984).
15. P. Yeh and C. Gu, *Optics of Liquid Crystal Displays* (Wiley, New York, 1999).
16. S. V. Pasechnik and A. V. Torchinskaya, *Mol. Cryst. Liq. Cryst.* **331**, 341 (1999).
17. I. Janossy, P. Pieranski, and E. Guyon, *J. Phys. (Paris)* **37**, 110 (1976).

Translated by N. Wadhwa